Performance Analysis of PLNC using Hierarchical Modulation

Safaa N. Awny, Charalampos C. Tsimenidis, Jonathon Chambers and Stephane Y. Le Goff
School of Electrical and Electronic Engineering, Newcastle University
Newcastle upon Tyne, NE1 7RU, UK
Email: {s.nash'at-awny; charalampos.tsimenidis; Jonathon.Chambers; stephane.le-goff}@newcastle.ac.uk

***Abstract*—In this paper, we propose and analyze the performance of a two-way relay network (TWRN) using physical layer network coding (PLNC) with hierarchical modulation (HM). The performance is evaluated for additive white Gaussian noise (AWGN) channels. The TWRN consists of two end nodes and a relay, where each node has a single antenna and operates in a half-duplex mode. Using an analytical approach, we derive the end-to-end symbol error rate (SER) performance expression of the 4/16-QAM HM for the high priority (HP) and the low priority (LP) streams, respectively, as a function of signal-to-noise ratio (SNR). It has been found the analytical and simulation results are in close agreement. The utilization of the proposed HM-PLNC system minimizes the computational complexity of the denoise and forward (DNF) operations at the relay by reducing the number of Euclidean distance computations required to 18 compared to the 49 required in an equivalent 16-QAM based PLNC system.**

***Index Terms*—Hierarchical modulation (HM), physical layer network coding (PLNC), denoise and forward (DNF), two-way relay network (TWRN), half-duplex (HD)**

I. Introduction

The first concept of the two-way relay network (TWRN) based on the principle of physical layer network coding (PLNC) was discussed in [1] as a novel method in order to raise spectral efficiency. The TWRN system consists of two end nodes, A and B, that exchange their information via a relay node, R, simultaneously. PLNC can potentially elevate the throughput of a traditional TWRN by 100 % [2], [3]. To relay information, PLNC can utilize various strategies at the relay, such as amplify-and-forward (AF) and denoise-and-forward (DNF) [4]. This paper focuses on the DNF scheme which has attracted much interest in recent research because it avoids noise amplification and can improve the achievable throughput [5].

The half-duplex (HD) operation in the denoise-and-forward physical layer network coding (DNF-PLNC) scheme consists of two phases; during the first phase, the two users send their messages simultaneously to the relay, which is known as the multiple access (MA) phase [6]. In the second phase, the relay broadcasts the superposed signals to the users, which is referred to as the broadcast (BC) phase. Research on PLNC so far focused on using binary or quaternary phase shift keying (BPSK, QPSK) modulation schemes resulting in 3 and 9 Euclidean distance computations (EDC) at the relay in an additive white Gaussian noise (AWGN) channel. In contrast, in fading channels, 4 and 16 EDC are theoretically required, respectively. Higher order modulations such as 16 quadrature amplitude modulation (QAM) can be used to further increase spectral efficiency, however, the complexity of implementation will be increased significantly at the relay at the DNF stage due to the 49 EDC required in AWGN, and the 256 EDC needed in fading channels.

To reduce the computation complexity of the DNF stage, we propose a PLNC scheme that utilizes hierarchical modulation (HM) or layered modulation [7], [8]. The idea of using HM is to merge two different bit streams into one single symbol, such as the high priority (HP) bit stream, which is used to select the quadrant, and the low priority (LP) stream to select the position inside the quadrant [9]. Utilizing HM enables a reduction in EDC at the relay, as only 18 EDC is required to detect both the HP and LP streams in the AWGN channel (9 per stream) and 32 EDC in fading channels. Thus, a significant reduction in the computation complexity of the DNF stage is achieved compared to 16-QAM.

The contributions of this paper can be summarized as follows: (i) The proposed HM-PLNC systems are presented to reduce the complexity preventing the utilization of a 16-QAM scheme. This is a novel approach and is completely different than the method outlined in [10], where HM was used asymmetrically in TWRC, such as the two end users can use either the HP or LP streams but not both; (ii) We optimize the HM parameters to achieve minimum symbol error rate (SER) and derive novel analytical expressions for the end-to-end SER for a 4/16-QAM system in the presence of AWGN. Approximate expressions for the SER of 4/16-QAM [11] and 4/M-QAM family for point-to-point links already exist [12], however, to the best of our knowledge, this is the first work that derives analytical end-to-end expression for an HM-PLNC system.

The remainder of the paper is organized as follows. Section II presents the system model combined with the uplink phase, DNF processing at the relay and broadcast phase. Section III provides the performance analysis in terms of end-to-end SER. Section IV shows the analytical and simulation results of the proposed system. Finally, Section V summaries the main conclusions of the paper.

ISBN 978-0-9928626-7-1 © EURASIP 2017

II. System Model

A. Uplink Phase

In this subsection, we introduce the uplink phase (UL) of the proposed HM-PLNC based system. A 4/16-QAM HM with Karnaugh map style, Gray-code mapping is depicted in Fig. 1. Per node, we assume that we have two incoming streams of information, one conveying the basic data stream (HP stream) and the other the enhancement data stream (LP stream). On every channel access, the HP bits, b_1 and b_2, along with the LP bits, b_3 and b_4, are sent to the signal mapper to obtain the output signal s_k^p as a transmitted signal for each user, where $p = \{A, B\}$ represents the two users A and B. It is noteworthy that the first two most significant bits (MSB), the HP bits, b_1 and b_2, select one of the four fictitious symbols of 4-QAM as illustrated in Fig. 2, controlling thus the quadrant selection. The remaining two least significant bits (LSB) identified as the LP bits, b_3 and b_4 denote the four symbols around the fictitious symbols in the in-phase (I) and quadrature-phase (Q). For the hierarchy of any symbol, three constellation distances

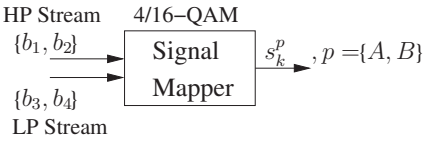

Fig. 1. Hierarchical Modulation for 4/16-QAM constellations.

are defined as d_1, d_2 and d_1' as depicted in Fig. 2. $2d_1$ denotes the distance between two constellation points belonging to the HP stream in different quadrants, while $2d_2$ represents the distance between two neighboring symbols within one quadrant. In addition, $2d_1'$ denotes the distance between two symbols in adjacent quadrants [10], [13]. Another parameter

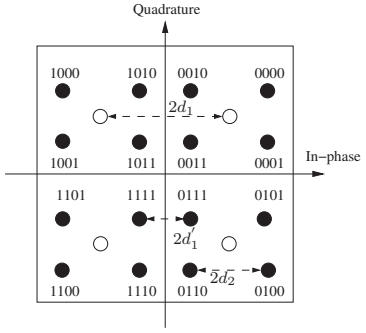

Fig. 2. Hierarchical constellation diagram of 4/16-QAM modulation.

used to characterize hierarchical constellations, referred to as the constellation robustness parameter, is defined as $\lambda = d_2/d_1$ and controls the balance of power between the HP and LP streams and the relative message priorities. In the case of 4/16-QAM, if λ = 0, the form is 4-QAM. In contrast, when $\lambda = \frac{1}{2}$ a 16-QAM constellation is constructed. Fig. 3 shows the block diagram of the proposed system and the diagram of the transmitters, denoted T_x, is illustrated in Fig. 1. The two users exchange their information via a relay node, however,

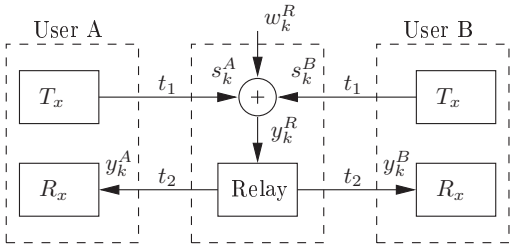

Fig. 3. Block diagram of TWRN with hierarchical modulation.

there is no direct connection between them. During the MA phase, the k-th received signal at the relay is given by

$$y_k^R = s_k^A + s_k^B + w_k^R, \tag{1}$$

where the two incoming HM type signals, such as $s_k^p, p \in \{A, B\}$ are constructed as

$$s_k^p = \mathbf{C}(b_k^{HP,p}) + \lambda \mathbf{C}(b_k^{LP,p}), \tag{2}$$

where $\mathbf{C} = [1 + j, -1 + j, 1 - j, -1 - j]^T$ is the 4-QAM constellation vector and λ is the robustness parameter. Furthermore, the m-ary symbols b_k^p are constructed as

$$b_k^{HP,p} = b_1 + 2b_2, \tag{3}$$

$$b_k^{LP,p} = b_3 + 2b_4, \tag{4}$$

where b_1, b_2, b_3 and $b_4 \in \{0, 1\}$. Finally, w_k^R represents the complex-valued AWGN samples with zero-mean and variance N_0, exhibiting a complex normal probability distribution, such as $\mathcal{CN}(0, N_0/2)$.

B. DNF at Relay Processing

In this subsection, we introduce the modified DNF scheme at the relay node for the TWRN channel that considers the HM type of transmitted signals. The relay detects the combination of HP and LP streams of both users as follows

$$\hat{b}_k^{HP} = \arg\min_m \left| y_k^R - \mathbf{C}^{PNC}(m) \right|, \tag{5}$$

$$\hat{b}_k^{LP} = \arg\min_m \left| y_k^R - \mathbf{C}^{PNC}(\hat{b}_k^{HP}) - \lambda \mathbf{C}^{PNC}(m) \right|, \tag{6}$$

where $\mathbf{C}_m^{PNC} = [2, 2 + 2j, +2j, 0, 2 - 2j, -2j, -2 + 2j, -2, -2 - 2j]^T$ is a vector containing all possible combinations of two independent 4-QAM symbols, and $m \in \{1, 2, \ldots, 9\}$. Subsequently, the PNC mapping constructs the transmitted signal for the downlink phase (DL) as

$$s_k^R = \mathbf{C}(f(\hat{b}_k^{HP})) + \lambda \mathbf{C}(\hat{b}_k^{LP}), \tag{7}$$

where $f(\hat{b}_k^{HP})$ denotes the denoise-and-forward mapping of the 9 points to compute the constellation.

C. Broadcast Phase

In the BC phase, the relay broadcasts s_k^R, which is received at the destination nodes as

$$y_k^p = s_k^R + w_k^p, \tag{8}$$

ISBN 978-0-9928626-7-1 © EURASIP 2017

where $p = \{A, B\}$ and w_k^p represents complex-valued, zero-mean AWGN noise samples with variance N_0. Finally, the end nodes extract the information transmitted by the source node as

$$\hat{b}_k^{HP,p} = \arg\min_m |y_k^p - \mathbf{C}(m)|, \tag{9}$$

$$\hat{b}_k^{LP,p} = \arg\min_m \left| y_k^p - \mathbf{C}(\hat{b}_k^{HP,p}) - \lambda \mathbf{C}(m) \right|. \tag{10}$$

III. Symbol Error Probability of Hierarchical 4/16-QAM Based PLNC

A. Symbol Error Probability at the Relay

Fig. 4 shows the noiseless constellation at the relay of the proposed system. Because the two users A and B send their data using 4/16-QAM HM, detection is composed of two detection stages. In the first stage, the HP points are detected for each 9-point cluster, while in the second stage the LP points surrounding the centre points are detected, as illustrated in (5) and (6) during the uplink phase and in (9) and (10) during the downlink phase, respectively. The complexity of the traditional 16-QAM constellation at the relay is relatively higher than that of the HM-PLNC system which shows a good performance with low computational complexity. The uplink symbol error probability is given as

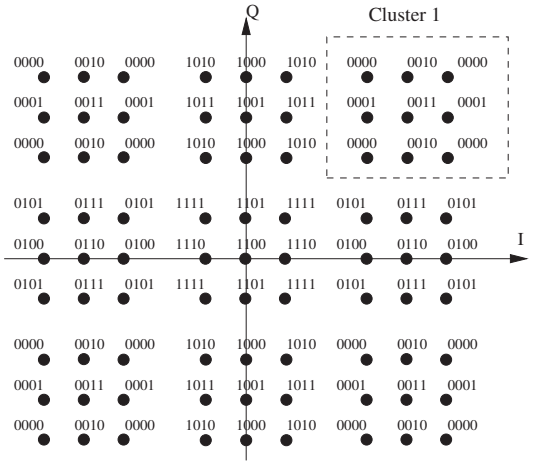

Fig. 4. Constellation diagram of 4/16-QAM HM at the Relay.

$$P_{UL} = \Pr\{S_m^{''} \neq S_m\}, \tag{11}$$

where P_{UL} represents the uplink symbol error probability, $\Pr\{\cdot\}$ the probability operator. $S_m^{''}$ and S_m denote the symbol detected by the receiver and the symbol actually transmitted, respectively, and m is the index which corresponds to a particular symbol in the constellation. As shown in Fig. 4, we can find the symbol error probability for 4/16-QAM HM-PLNC scheme for the area labelled as cluster 1, assuming that the probability density function (PDF), $f(.)$, of the real part of y_k^R, $\Re\{y_k^R\}$, is given as

$$f(\Re\{y_k^R\}|S_{m,n}) = \frac{1}{\sqrt{2\pi\sigma^2_{\Re\{y_k^R\}}}} e^{-\frac{(\Re\{y_k^R\} - \Re\{S_{m,n}\})^2}{2\sigma^2_{\Re\{y_k^R\}}}}, \tag{12}$$

where $\sigma^2_{\Re\{y_k^R\}}$ represents the variance of the real part of y_k^R, and m , $n \in \{1, 2, ..., 9\}$ represent the cluster number and the constellation order inside the cluster, respectively. As we can see the dashed area in Fig. 4, expanded for clarity in Fig. 5, the symbol $S_{1,1} = 0000$ on the top right point, which represents symbol 1, is decoded correctly only if y_k^R falls in the decision region described as

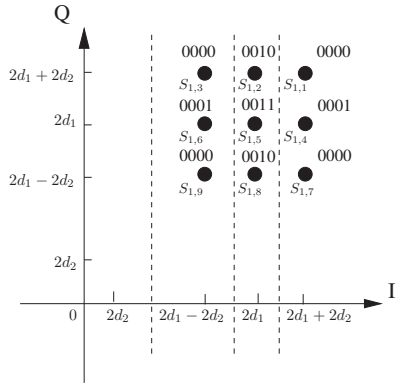

Fig. 5. Decision boundaries for cluster 1 hierarchical modulation.

$$P_c(y_k^R|S_{1,1}) = P_c\left(\Re\{y_k^R\} \geq 2d_1 + d_2\right) \times P_c\left(\Im\{y_k^R\} \geq 2d_1 + d_2\right), \tag{13}$$

where P_c is the probability of correctly detecting symbol 1 in cluster 1, and the operators $\Re\{y_k^R\}$ and $\Im\{y_k^R\}$ denote the real and imaginary parts of y_k^R, respectively. Due to symmetry, the marginal probabilities for the real and imaginary components are equal for $S_{1,1}$. Therefore, the P_C of the real component of y_k^R is given by

$$P_c(\Re\{y_k^R\}|\Re\{S_{1,1}\}) = \frac{1}{\sqrt{2\pi\sigma^2_{\Re\{y_k^R\}}}} \times \int_{2d_1+d_2}^{\infty} e^{-\frac{(\Re\{y_k^R\} - \Re\{S_{m,n}\})^2}{2\sigma^2_{\Re\{y_k^R\}}}} d\Re\{y_k^R\}, \tag{14}$$

by substituting

$$\frac{u^2}{N_0} = \frac{(\Re\{y_k^R\} - \Re\{S_{m,n}\})^2}{2\sigma^2_{\Re\{y_k^R\}}}, \tag{15}$$

the expression for the differential element $d\Re\{y_k^R\}$ as

$$d\Re\{y_k^R\} = \frac{1}{\sqrt{2\pi\sigma^2}}\, d_u, \tag{16}$$

and the upper integration limit as, $u = -d_2$, where $2d_1 + d_2$ is the lower bound in the real and the imaginary axis, respectively. By substituting (15) and (16) in (14), we can rewrite (14) as

$$P_c(\Re\{y_k^R\}|\Re\{S_{1,1}\}) = \frac{1}{\sqrt{\pi N_0}} \int_{-d_2}^{\infty} e^{\frac{-u^2}{N_0}}\, du. \tag{17}$$

ISBN 978-0-9928626-7-1 © EURASIP 2017

By introducing the expression for the complementary error function $\mathrm{erfc}(\cdot)$ [14, eq.(8.250.4)] defined as

$$\mathrm{erfc}(x) = \frac{2}{\sqrt{\pi}} \int_{x}^{+\infty} e^{-u^2}\, du, \tag{18}$$

and replacing the variable u with $t\sqrt{N_0}$, we can re-write (17) as

$$P_c(\Re\{y_k^R\}|\Re\{S_{1,1}\}) = 1 - \frac{1}{2}\mathrm{erfc}\Big(\frac{d_2}{\sqrt{N_0}}\Big). \tag{19}$$

Similarly, due to the symmetry, the probability of correctly detecting the imaginary component of y_k^R is given by

$$P_c(\Im\{y_k^R\}|\Im\{S_{1,1}\}) = 1 - \frac{1}{2}\mathrm{erfc}\Big(\frac{d_2}{\sqrt{N_0}}\Big). \tag{20}$$

Finally, the symbol error probability is then given as [15]

$$P_s(y_k^R|S_{1,1}) = 1 - P_c(y_k^R|S_{1,1}). \tag{21}$$

By substituting (13), (19) and (20) in (21), the symbol error probability of $S_{1,1}$ is approximated as

$$P_s(y_k^R|S_{1,1}) = \mathrm{erfc}\Big(\frac{d_2}{\sqrt{N_0}}\Big) - \frac{1}{4}\mathrm{erfc}^2\Big(\frac{d_2}{\sqrt{N_0}}\Big). \tag{22}$$

Due to the constellation symmetry in cluster 1, following a similar approach, we can compute the symbol error probability of the following pair points ($S_{1,2}$ and $S_{1,4}$), ($S_{1,3}$ and $S_{1,7}$) and ($S_{1,6}$ and $S_{1,8}$). In addition, $S_{1,5}$ and $S_{1,9}$ are unique. Nevertheless, due to space limitations the derivations are omitted here for the other points in cluster 1 and other clusters.

Using Bayes' rule, the overall symbol error probability for the uplink can be written as [15]

$$\mathrm{P}_{UL}^{q} \approx \sum_{m=1}^{M} \sum_{S_n \in Z_m} P_s^q\{S_{m,n}\} P_s\{S_m\}, \tag{23}$$

where $P_s^q\{S_{m,n}\}$ denotes the probability to detect $S_{m,n}$ given that S_m was transmitted and Z_m is the set containing all the nearest neighbour symbols of S_m. $q = \{\mathrm{HP}, \mathrm{LP}\}$, representing the HP and LP streams, respectively. Since all symbols are transmitted with equal probabilities, $P_s\{S_m\} = \frac{1}{M}$, where M denotes the constellation size. Finally, we have the final symbol error rate (SER) expression to determine P_{UL}^q for the HP and LP uplink phase as follows

$$\mathrm{P}_{UL}^{q} \approx \frac{1}{M} \sum_{m=1}^{M} \sum_{S_n \in Z_m} P_s^q\{S_{m,n}\}, \tag{24}$$

B. Downlink Symbol Error Probability

After y_k^p has been mapped using PNC at the relay, it is broadcast to both users A and B simultaneously at the second time slot, which decode y_k^p to determine $\hat{b}_k^{\mathrm{HP},p}$ and $\hat{b}_k^{\mathrm{LP},p}$ as mentioned in (9) and (10). In the case of hierarchical modulation, the two streams, HP and LP, are independent, thus, we will calculate the asymptotic SER of each stream. In the case of square 4/16-QAM, the data bits are divided into two sub-channels, for the real and imaginary parts. Both sub-channels have the same average error probability, therefore, the latter can be computed using only the real or the imaginary sub-channel. Therefore, we show the SER derivation for the real sub-channel, $\Re\{y_k^p\}$, only as illustrated in Fig. 2 that depicts a simplified diagram of 4/16-QAM. We can express the error probability of the HP stream of the HP stream of the virtual 4-QAM constellation can be given as [12], [16]

$$\mathrm{P}_{DL}^{HP} \approx \frac{1}{4}\mathrm{erfc}\Big(\frac{d_1+d_2}{\sqrt{N_0}}\Big) + \frac{1}{4}\mathrm{erfc}\Big(\frac{d_1-d_2}{\sqrt{N_0}}\Big), \tag{25}$$

which can be rewritten using λ as

$$\mathrm{P}_{DL}^{HP} \approx \frac{1}{4}\mathrm{erfc}\Big(\frac{1+\lambda}{\sqrt{1+\lambda^2}}\sqrt{\mathrm{SNR}}\Big) + \frac{1}{4}\mathrm{erfc}\Big(\frac{1-\lambda}{\sqrt{1+\lambda^2}}\sqrt{\mathrm{SNR}}\Big). \tag{26}$$

As illustrated in Fig. 2, the error probability of the LP stream of the constellation points of the real sub-channel can be calculated as

$$\mathrm{P}_{DL}^{LP} \approx \mathrm{erfc}\Big(\frac{d_2}{\sqrt{N_0}}\Big) + \frac{1}{2}\mathrm{erfc}\Big(\frac{2+d_2}{\sqrt{N_0}}\Big) - \frac{1}{2}\mathrm{erfc}\Big(\frac{2-3d_2}{\sqrt{N_0}}\Big), \tag{27}$$

which can be re-written using λ as

$$\mathrm{P}_{DL}^{LP} \approx \mathrm{erfc}\Big(\frac{\lambda}{\sqrt{1+\lambda^2}}\sqrt{\mathrm{SNR}}\Big) + \frac{1}{2}\mathrm{erfc}\Big(\frac{2+\lambda}{\sqrt{1+\lambda^2}}\sqrt{\mathrm{SNR}}\Big) - \frac{1}{2}\mathrm{erfc}\Big(\frac{2-3\lambda}{\sqrt{1+\lambda^2}}\sqrt{\mathrm{SNR}}\Big). \tag{28}$$

C. END-to-END Performance

The end-to-end performance of 4/16-QAM HM is considered in the presence of AWGN for mid to high SNR levels that result in the following assumptions: (i) Correctly detected bits at the relay during the MA phase are detected incorrectly at the end nodes during the BC phase (ii) Bit errors at the relay are detected with no error at the end nodes during the BC phase. Thus, for the end-to-end (E2E) SER performance can be given as

$$\mathrm{P}_{E2E}^{HP} \approx (1 - \mathrm{P}_{UL}^{HP})\mathrm{P}_{DL}^{HP} + (1 - \mathrm{P}_{DL}^{HP})\mathrm{P}_{UL}^{HP}, \tag{29}$$

$$\mathrm{P}_{E2E}^{LP} \approx (1 - \mathrm{P}_{UL}^{LP})\mathrm{P}_{DL}^{LP} + (1 - \mathrm{P}_{DL}^{LP})\mathrm{P}_{UL}^{LP}, \tag{30}$$

where P_{UL}^{HP}, P_{DL}^{HP}, P_{UL}^{LP} and P_{DL}^{LP} are the symbol error probabilities for the uplink and the downlink of HP and LP streams, respectively.

IV. NUMERICAL RESULTS

This section presents analytical and simulation results for the TWRN based on the proposed HM-PLNC approach. The analytical E2E SER expressions derived in this paper have been verified by Monte Carlo simulations to assess the performance of the proposed HM-PLNC system. We consider an HD-TWRN network, where half-duplex users A and B exchange data with the aid of a DNF half-duplex relay node R over AWGN channels. Fig. 6 shows the effect of the variation of λ on the performance of the proposed HM-PLNC based

ISBN 978-0-9928626-7-1 © EURASIP 2017

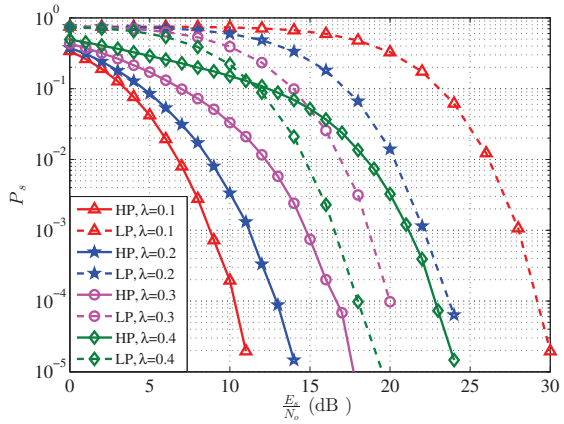

Fig. 6. Effect of the variation of λ of the SER performance over AWGN.

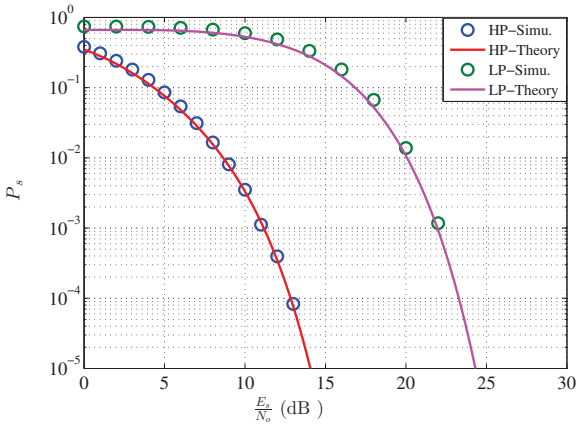

Fig. 7. Effect of AWGN on the SER performance of 4/16-QAM with λ = 0.2.

TWRN, where the E2E SER of the HP and LP streams are investigated. We have evaluated systematically the E2E SER for different values of λ in the range of 0.1-0.4, and investigated its influence on the performance of the proposed system. The optimal value of λ for the AWGN channel is 0.2. This value minimizes the total E2E SER of the two information streams, i.e. HP and LP. A closer look at the figure reveals that for λ= 0.1 the HP stream exhibits a low E2E SER. However, in this case, a high SNR is required to obtain acceptable E2E SER for the LP stream. In contrast, large values of λ result in poor SER performance for the HP stream. We have generated 10^7 bits of data to test the proposed system in the SNR range of 0-30 dB for HP and LP streams. Fig. 7 shows that for high SNR the analytical and empirical results for the E2E SER performance of the proposed HM-PLNC system are closely matched for both the HP and LP streams. The observations show that the E2E SER value of the enhancement bits increases by decreasing the ratio λ, since the Euclidean distance of the constellation points is reduced.

V. CONCLUSION

In this paper, we propose a half-duplex HM-PLNC system to improve spectral efficiency of TWRN while keeping the DNF complexity at the relay low. It is found that the combination of 16-QAM constellations and half-duplex PLNC systems increases the system complexity at the relay node. To tackle this disadvantage, the HM scheme was introduced as a proposed solution according to the value of λ. To this end, we derived the asymptotic expression for the constellations at the relay (the uplink) to calculate the SER probability in the MA phase; and later we derived the end-to-end SER of the HP and LP streams. The analytical derived expressions have been verified with Matlab Monte Carlo simulations. It was found that both simulation and analytical results are in a good agreement in the high SNR regime. Future work will focus on performance of the proposed system in fading channels.

REFERENCES

[1] S. Zhang, S. C. Liew, and P. P. Lam, "Hot topic: Physical-layer network coding," in *Proc. of the 12th Annu. Int. Conf. on Mobile Computing and Networking*, ser. MobiCom '06. New York, NY, USA: ACM, 2006, pp. 358–365.

[2] Q. Huo, K. Yang, L. Song, Y. Li, and B. Jiao, "Compressed relaying for two-way relay networks with correlated sources," *IEEE Wireless Commun. Lett.*, vol. 4, no. 1, pp. 30–33, Feb 2015.

[3] L. Lu, L. You, Q. Yang, T. Wang, M. Zhang, S. Zhang, and S. C. Liew, "Real-time implementation of physical-layer network coding," in *Proc. of the 2nd Workshop on Software Radio Implementation Forum*. ACM, 2013, pp. 71–76.

[4] V. Namboodiri, K. Venugopal, and B. S. Rajan, "Physical layer network coding for two-way relaying with QAM," *IEEE Trans. on Wireless Commun.*, vol. 12, no. 10, pp. 5074–5086, October 2013.

[5] Y. Huang, S. Wang, Q. Song, L. Guo, and A. Jamalipour, "Synchronous physical-layer network coding: A feasibility study," *IEEE Trans. on Wireless Commun.*, vol. 12, no. 8, pp. 4048–4057, August 2013.

[6] S. Zhang and S. C. Liew, "Applying physical-layer network coding in wireless networks," *EURASIP Journal on Wireless Commun. and NetWork.*, vol. 2010, p. 1, 2010.

[7] R. Ahmad and M. O. Hasna, "Joint hierarchical modulation and network coding for two way relay networks," in *Vehicular Technology Conf. (VTC Spring), 2012 IEEE 75th*, May 2012, pp. 1–6.

[8] C. Hausl and J. Hagenauer, "Relay communication with hierarchical modulation," *IEEE Commun. Lett.*, vol. 11, no. 1, pp. 64–66, Jan 2007.

[9] H. Méric and J. M. Piquer, "DVB-S2 spectrum efficiency improvement with hierarchical modulation," in *2014 IEEE International Conference on Communications (ICC)*. IEEE, 2014, pp. 4331–4336.

[10] J. M. Park, S. L. Kim, and J. Choi, "Hierarchically modulated network coding for asymmetric two-way relay system," *IEEE Trans. on Vehicular Technology*, vol. 59, no. 5, pp. 2179–2184, Jun 2010.

[11] M. Morimoto, H. Harada, M. Okada, and S. Komaki, "A study on power assignment of hierarchical modulation schemes for digital broadcasting," *IEICE Trans. on Commun.*, vol. 77, no. 12, pp. 1495–1500, 1994.

[12] P. K. Vitthaladevuni and M.-S. Alouini, "BER computation of 4/M-QAM hierarchical constellations," *Broadcas., IEEE Trans. on*, vol. 47, no. 3, pp. 228–239, Sep. 2001.

[13] B. Mouhouche, A. Mourad, and D. Ansorregui, "Throughput optimization of precoded ofdm with hierarchical modulation," in *2013, 7th International Conference on Signal Processing and Communication Systems (ICSPCS)*, Dec 2013, pp. 1–10.

[14] I. S. Gradshteyn and I. M. Ryzhik, *Tables of Integrals, Series, and Products*, 7th ed. Academic Press, 2007.

[15] J. Proakis, *Digital Communications*, ser. Electrical engineering series. McGraw-Hill, 2001.

[16] H. Jiang and P. A. Wilford, "A hierarchical modulation for upgrading digital broadcast systems," *IEEE Transactions on Broadcasting*, vol. 51, no. 2, pp. 223–229, June 2005.

ISBN 978-0-9928626-7-1 © EURASIP 2017